Wear Particles from Studded Tires and Granite Pavement Induce Pro-inflammatory Alterations in Human Monocyte-Derived Macrophages: A Proteomic Study

ARTICLE *in* CHEMICAL RESEARCH IN TOXICOLOGY · JANUARY 2011

Impact Factor: 3.53 · DOI: 10.1021/tx100281f · Source: PubMed

7 AUTHORS, INCLUDING:

Helen m Karlsson
University Hospital Linköping
28 PUBLICATIONS **443** CITATIONS
SEE PROFILE

Bijar Ghafouri
Linköping University
54 PUBLICATIONS **604** CITATIONS
SEE PROFILE

Mats Lindahl
Linköping University
65 PUBLICATIONS **1,816** CITATIONS
SEE PROFILE

Anders G Ljungman
Linköping University
23 PUBLICATIONS **638** CITATIONS
SEE PROFILE

Wear Particles from Studded Tires and Granite Pavement Induce Pro-inflammatory Alterations in Human Monocyte-Derived Macrophages: A Proteomic Study

Helen Karlsson,[†,‡] John Lindbom,[†] Bijar Ghafouri,[†,‡,#] Mats Lindahl,[†] Christer Tagesson,[†,‡] Mats Gustafsson,[§] and Anders G. Ljungman*[,†]

Division of Occupational and Environmental Medicine, Department of Clinical and Experimental Medicine, Faculty of Health Sciences, SE-581 85 Linköping University, Sweden, Division of Occupational and Environmental Medicine and Division of Pain and Rehabilitation, University Hospital, SE-581 85 Linköping, Sweden, and Swedish National Road and Transport Research Institute (VTI), SE-581 95 Linköping, Sweden

Received August 16, 2010

Airborne particulate matter is considered to be one of the environmental contributors to the mortality in cancer, respiratory, and cardiovascular diseases. For future preventive actions, it is of major concern to investigate the toxicity of defined groups of airborne particles and to clarify their pathways in biological tissues. To expand the knowledge beyond general inflammatory markers, this study examined the toxicoproteomic effects on human monocyte derived macrophages after exposure to wear particles generated from the interface of studded tires and a granite-containing pavement. As comparison, the effect of endotoxin was also investigated. The macrophage proteome was separated using two-dimensional gel electrophoresis. Detected proteins were quantified, and selected proteins were identified by matrix-assisted laser desorption/ionization time of flight mass spectrometry. Among analyzed proteins, seven were significantly decreased and three were increased by exposure to wear particles as compared to unexposed control cells. Endotoxin exposure resulted in significant changes in the expression of six proteins: four decreased and two increased. For example, macrophage capping protein was significantly increased after wear particle exposure only, whereas calgizzarin and galectin-3 were increased by both wear particle and endotoxin exposure. Overall, proteins associated with inflammatory response were increased and proteins involved in cellular functions such as redox balance, anti-inflammatory response, and glycolysis were decreased. Investigating the effects of characterized wear particles on human macrophages with a toxicoproteomic approach has shown to be useful in the search for more detailed information about specific pathways and possible biological markers.

Introduction

The mortality in cancer, respiratory, and cardiovascular diseases is the major cause of a shortened life span in the industrialized part of the world. Among the environmental factors contributing to these pathologies is airborne particulate matter (PM[1]) (*1, 2*). The PM fractions are usually divided in three categories: ultrafine (<0.1 μm in diameter), fine (0.1−2.5 μm), and coarse (2.5−10 μm), the coarser mode seemingly more associated with acute airway symptoms and the finer mode with cardiovascular disease. Apart from size, the toxicological properties of the particles are dependent on several factors such as chemical composition, shape, and adsorbed material (*3, 4*). The concentration of PM in the air at a given location is dependent on contributions from long-range transport as well as local sources. Contributing factors among others are combustion emissions (*5*), mineral dust (*6*), winter sanding of the roads (*7*), and volcanic eruptions (*8*). Lately, wear particles (WP) generated from traffic have been recognized as a major contributing source to the overall PM load, especially in Nordic countries where studded tires are used in the winter and many WP are generated at the interface between the tires and the road surface (*7*). Accordingly, there is now serious concern about the health effects of WP from studded tires and the underlying mechanisms by which they exert their toxic actions.

Previous studies have demonstrated that PM has a wide range of pro-inflammatory effects in various experimental systems. For example, a number of investigations employing human or murine macrophages have demonstrated increased release of cytokines, oxidative stress, and apoptosis after exposure to PM (*9*−*11*). In addition, exposures of human and canine alveolar macrophages to PM have been demonstrated to result in the generation of arachidonic acid, prostaglandin E_2, and leukotriene B_4 through cytosolic phospholipase A_2-dependent activation (*12*). We have previously shown that WP from studded tires are able to induce a number of pro-inflammatory events in macrophages, such as secretion of interleukin-6, interleukin-8, and tumor necrosis factor-α from human monocyte-derived macrophages and induction of lipid peroxidation, nitric oxide formation, and arachidonic acid release from murine RAW 264.7 macrophages (*13, 14*). These findings illustrate that WP from

* Author to whom correspondence should be addressed (phone +46-10-1031481; e-mail anders.ljungman@liu.se).

† Division of Occupational and Environmental Medicine, Department of Clinical and Experimental Medicine, Faculty of Health Sciences.

‡ Division of Occupational and Environmental Medicine, University Hospital.

Division of Pain and Rehabilitation, University Hospital.

§ Swedish National Road and Transport Research Institute (VTI).

[1] Abbreviations: PM, particulate matter; WP, wear particles; MDM, monocyte-derived macrophages; 2-DE, two-dimensional gel electrophoresis; SDS-PAGE, sodium dodecyl sulfate−polyacrylamide gel electrophoresis; MALDI TOF MS, matrix-assisted laser desorption ionization time of flight mass spectrometry; SEM, scanning electron microscopy; EDX, emission dispersive X-ray spectroscopy.

10.1021/tx100281f
Published on Web 11/30/2010

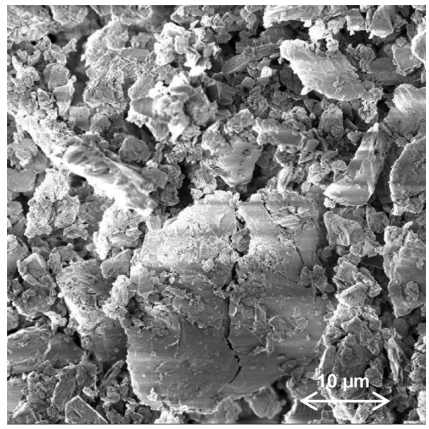

Figure 1. SEM image of the particles, at a magnification of 2000×.

studded tires have considerable pro-inflammatory potential and profound effects on macrophages in vitro, although many details of their action remain to be clarified. It is also well-known that PM is able to interact with endotoxins (ETX) (*15*); thus, the objective of this study was to search for more specific biomarkers of WP toxicity that would help to distinguish the effect of WP in vitro and perhaps even in vivo from that of other pro-inflammatory agents. The ability to do so would be of significant value in the elucidation of the mechanisms behind WP-induced health risks.

In the present investigation, we have used two-dimensional gel electrophoresis (2-DE) and mass spectrometry (MS) to examine the effects of WP, with no measurable amounts of ETX, generated from the interaction of studded tires and granite pavement, on the proteome of human monocyte-derived macrophages (MDM). In addition, the effects of ETX on the MDM proteome were examined and compared to those of WP. The results obtained indicate that a toxicoproteomic approach is a useful tool in the search for more detailed information about the interaction between particles and human macrophages.

Materials and Methods

Particle Generation and Characterization. The WP were generated, sampled, and characterized as previously described (*7*). Briefly, a road simulator (at the Swedish National Road and Transport Research Institute, VTI) was used to generate the WP from the tire/pavement interface. For this investigation a common road surface material in Sweden, dense asphalt with granite (asphalt containing granite as the major stone material) was used. Studded tires were used, and the speed of the wheels was 70 km/h. The generated particles were collected using a high-volume sampler designed to collect the PM_{10} fraction (Sierra-Andersen/GMW model 12000) equipped with glass fiber filters (Munktell MG 160). The mass and size distribution was measured with an aerodynamic particle sizer and showed to be bimodal with peaks around 4−5 and 7−8 μm. Whereas the WP within these sizes constitute the majority of the sample mass, the number of ultrafine particles that were formed during the trials exceeds the other particle fractions, with the dominant number distribution of ultrafine particles of about 40 nm, which was measured using a Scanning Mobility Particle Sizer system (SMPS). Scanning electron microscopy (SEM) analysis (Figure 1) gave strong indications that a totally dominating part of the coarser particle fraction (1−10 μm) is mineral particles, which were flaky in their appearance. Silica was the dominating peak in the emission dispersive X-ray spectroscopy (EDX) spectrum in Figure 2. Analysis showed the mineral content to be amorphous and to contain as percent of weight 30.3 ± 0.9 SiO_2, 35.2 ± 1.2 $KAlSi_3O_8$, and 34.5 ± 1.2 $NaAlSi_3O_8$. The particles were recovered from the filters by shaking, as the level of the material was very high. No ETX was detected using Endotoxate (Sigma), which has a lowest detectable amount of 0.006 ng/mL according to the manufacturer, and no E-TOXATE inhibitor was present.

Cell Cultures. Human monocytes were isolated from heparinized human whole blood and allowed to differentiate into macrophages (MDM) as previously described (*14*). Briefly, on top of 20 mL of Polymorphprep (Axis Shield, Oslo, Norway) was added 5 mL of Lymphoprep to form a gradient, to which 25 mL of whole blood was added. The samples were centrifuged at room temperature in a swing-out rotor at 480*g* for 40 min. This resulted in separation of the leukocytes in two bands, with the upper band just below the plasma consisting of mononuclear leukocytes. The monocytes were transferred to a new 50 mL tube (Costar, Cambridge, MA), which was filled with cold Krebs−Ringer glucose (KRG) without Ca^{2+} and centrifuged 480*g* for 10 min at 4 °C. The supernatant was discarded and the pellet suspended in 5 mL of KRG without Ca^{2+} and centrifuged 250*g* for 7 min at 4 °C to remove the platelets. The pellet was then suspended in 2 mL of Macrophage-SFM medium (Invitrogen, Carlsbad, CA) supplemented with antibiotics (100 U/mL penicillin and 100 μg/mL streptomycin, Invitrogen). The cells were counted in a Bürker chamber, and approximately 15 million cells/25 cm^2 vial were shown out and allowed to adhere for 1 h in a cell incubator (Galaxy, Biotech, Northants, U.K.) at 37 °C and 5% CO_2. Thereafter, the cells were washed with 37 °C KRG with Ca^{2+} until no loose cells remained. After 10 days of incubation, the monocytes had morphologically derived into macrophages. The number of monocytes that had differentiated to macrophages varied between 100 000 and 200 000 cells/25 cm^2 vial.

The cells were counted with a grid ocular (Zeiss) at 20× magnification. Using this magnification the grid represents a square area of 0.0025 cm^2 (one vial of 25 cm^2 includes 10 000 such squares).

Cell Exposure and Protein Extraction. Prior to exposure, the cells were washed three times with PBS I and then incubated for 30 min with RPMI 1640 (Invitrogen) protein-free medium with antibiotics (100 U/mL penicillin and 100 μg/mL streptomycin, Invitrogen). Then, the medium was removed and replaced with new medium containing the stimuli. The particles were resuspended in the cell medium and sonicated using a Soniprep 150 (MSE, Leicestershire, U.K.) set at 14 μm 2 × 10 s. The cells were then incubated with a final concentration of 100 μg/mL of WP, the concentration used for ETX (LPS). (*Escherichia coli*, Sigma Chemical Co., St. Louis, MO) exposure was 10 μg/mL. As controls, macrophages exposed to cell medium only were used. The cells were incubated for 18 h in a total volume of 1.5 mL/vial. To ensure that the derived macrophages were responsive to stimuli, the

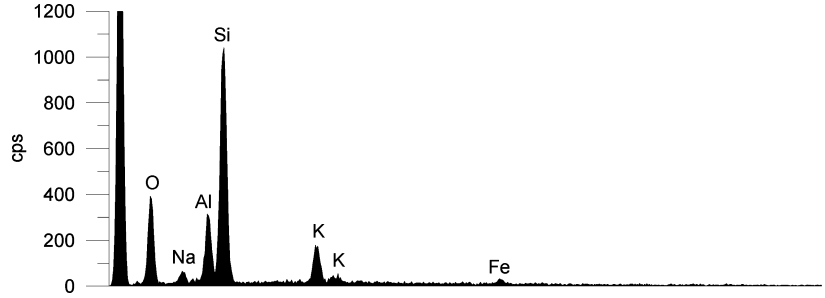

Figure 2. EDX spectra of the particles; expressed as cps, counts/s.

secretion into the medium of IL-6 and TNF-α after exposure to ETX was measured using the QuantiGlo system according to the manufacturer's instructions (R&D Systems, Minneapolis, MN). The detection limits were <0.2 pg/mL (linearity from 0.3 to 3000 pg/mL) and 0.45 pg/mL (linearity from 2.2 to 7000 pg/mL) for IL 6 and TNF-α, respectively. ETX exposure resulted in 300- and 16-fold increases in the amounts of IL 6 and TNF-α, respectively, in the medium as compared to unstimulated control cells.

After the exposure, the cell medium was removed and the cells were washed three times with 25 mM Tris, pH 7.4 (37 °C). Then 1 mL (0.5 mL) of a protease inhibitor cocktail consisting of 50 mM Tris/cocktail tablet (Roche, Basel, Switzerland), 9.4 mM EDTA, 65 mM dithiotreitol (DTT), 0.5 mg/mL DNase (Roche), and 0.2 mg of RNase (Roche) was added, and the cells were detached by scraping and transferred to Eppendorf tubes, sonicated at 14 μm 2 × 10 s, and incubated for 1 h at room temperature before centrifugation at 3000*g* and 4 °C for 20 min to remove cell membranes and ingested/adsorbed WP. Five microliters of the supernatant was removed and used for measuring the protein concentration using a color reagent (Bio-Rad) and measured at 595 nm using a Beckman Coulter DU800 spectrophotometer. The rest of the supernatant was then precipitated with nine parts of 10% trichloroacetic acid in acetone with 20 mM DTT per part of supernatant and incubated at −20 °C for 2 h. The tubes were centrifuged at 4 °C and 19800*g* for 5 min, the supernatant was removed, and the pellet was washed twice with 4 °C 20 mM DTT in acetone, centrifuged at 4 °C and 19800*g* for 5 min, and stored at −20 °C until analysis.

Analysis of Cell Viability. The viability of the cells was analyzed using the Trypan blue (Merck, Rahway, NJ) method. The cells were incubated for 15 min in the cell incubator with a 1:1 dilution of 0.1% trypan blue and phosphate-buffered saline (PBS I), after which the cells were washed three times with PBS I to remove excess Trypan blue before evaluation of the viability. No statistical difference was seen in the viability of unexposed control cells (96 ± 1.0%) as compared to cells exposed to WP (91 ± 1.0%) or ETX (96 ± 1.0%).

2-DE Analysis. 2-DE was performed using IPGphor and Multiphor (Amersham Bioscience, Uppsala, Sweden) as described previously (*16*). Briefly, the proteins were resuspended in 150 μL of a sample buffer containing 9 M urea, 65 mM DTT, 2% Pharmalyte (Amersham), 4% (3-(3-cholamidopropyl)dimethylammino)-1-propanesulfonate (CHAPS), and 1% bromophenol blue and then centrifuged at 4 °C and 23000*g* for 30 min to remove debris. The supernatant was mixed with a rehydration buffer consisting of 8 M urea, 4% CHAPS, 0.5% IPG buffer 3−10 NL (GE Health Care, Bioscience, Uppsala, Sweden), 19 mM DTT, and 5.5 mM Orange G to a final volume of 350 μL. The first dimension was performed by applying the samples in-gel rehydration for 12 h in 30 V and pH 3−10 nonlinear IPGs. The proteins were then focused at 53000 Vh at a maximum voltage of 8000 V. The second dimension (SDS-PAGE) was performed by transferring the p*I* focused proteins (IPGs) to homogeneous gels with a density of $T = 14\%$ and cross-linking of $C = 1.5\%$. The electrophoresis was performed at 40−800 V, 10 °C, 20−40 mA, overnight.

Silver Staining and Image Analysis. The gels were silver stained using the method described by Shevchenko et al. (*17*). Gray-scale images of the protein patterns were created and analyzed using a CCD camera and Fluor-S Multi-imager (Bio-Rad) in combination with an imaging analysis program PDQuest 7.0 (Bio-Rad). Images were evaluated by spot detection and intensities. Proteins were quantified as optical density per total protein intensity (ppm) on the 2-D gels. All evaluations done in the PDQuest program were done as five different comparisons. Four comparisons consisted of three gels representing the proteins isolated from control and WP- and ETX-exposed MDM cells, respectively. One comparison consisted of proteins from control and ETX-exposed cells. The gels (control, WP, and ETX) used in each comparison represent one cell exposure occasion consisting of control (unexposed cells) and WP- and ETX-exposed cells performed at the same time using cells from the same donor. After the gray scale images had been created, the gels were stored in plastic bags with Milli-Q water at 5 °C until further analysis.

Isolation of Protein Spots. Protein spots were excised from the gels using a syringe and transferred to Eppendorf tubes. Twenty-five microliters of 100 mM sodium thiosulphate and 25 μL of potassium ferricyanide were added to the gel pieces for destaining. When the pieces were completely destained, the chemicals were removed by washing (6 × 5 min with Milli-Q water) before the addition of 50 μL of 200 mM ammonium bicarbonate and incubation for 20 min at room temperature. The gel pieces were washed (3 × 5 min with Milli-Q water) and dehydrated with 100% acetonitrile for 5 min or until the gel pieces were opaque white. After removal of the acetonitrile, the gel pieces were dried in a SpeedVac vacuum concentration system (Savant, Farmingdale, NY). Twenty-five microliters of trypsin (Promega, Madison, WI) (10 μg/mL in 25 mM ammonium bicarbonate) was added, and the samples were incubated on ice for 30 min to allow the trypsin to be absorbed into the dried gel pieces. The samples were then incubated at 37 °C overnight. The peptide-containing supernatant was then transferred to new Eppendorf tubes, and 50 μL of 50% acetonitrile with 5% triflouracetic acid (TFA) was added and incubated at room temperature for 5 h with constant shaking. The supernatants were pooled and dried in a SpeedVac.

Mass Spectrometry. The dried peptides were resolved in 5 μL of 0.1% TFA and mixed in a 1:1 ratio with the matrix (0.19 M 2,5-dihydroxybenzoic acid, Fluka, Buchs, Switzerland) dissolved in 70% acetonitrile with 0.3% TFA. One microliter of the mixture was then applied on a stainless steel target plate. External calibration was performed using a standard protein mix (des-Arg-bradykinin (*m*/*z* 904.468), angiotensin I (*m*/*z* 1296.6853), Glu 1-fibrinopeptide B (*m*/*z* 1570.6447), adrenocorticotropic hormone clip 1−17 (*m*/*z* 2093.0867), and ACTH clip 18−39 (*m*/*z* 2465.1989), Applied Biosystems, Foster City, CA). Peptide mass fingerprinting was performed with MALDI-TOF (Voyager DE PRO, Applied Biosystems) with a 337 nm N_2 laser. The instrument was adjusted to a reflecting operating mode and a delayed extraction of 170 ns, to increase the resolution. The accelerating voltage used was 20000 V with a voltage grid of 79%. The intensity of the laser was set to 2501, and the mass range collected was 600−3600 Da. Data processing of the spectra was performed by Data Explorer version 4.0 (Applied Biosystems). Internal calibration was achieved using known trypsin autolysis peaks (*m*/*z* 842.5100 and 2211.1046) prior to database search.

Database Search. The major peaks in the spectra were submitted to database search using Swiss-Prot and NCBI with MS-Fit as the search engine (http:\\prospector.ucsf.edu). The search performed had the following restrictions: *Homo sapiens*, mass tolerance < 100 ppm, cysteines modified by carbamidomethylation, and a maximum of one missed cleavage by trypsin.

Statistical Analysis. Protein intensity values (ppm) from the quantification procedure representing five control (unexposed cells), five ETX-, and four WP-exposed cell experiments were transferred to the SPSS statistical analysis software, and differences in protein expression between control cells and WP-exposed or ETX-exposed cells, respectively, were evaluated by Mann−Whitney nonparametric test for unpaired samples. A p value of <0.1 was considered to be significant.

Results

A representative 2-DE pattern of the human MDM proteome is shown in Figure 3. Altogether 626 protein spots were detected and compared for intensity in control and WP- and ETX-exposed cells. Of these, 119 were identified by MALDI TOF MS (Table 1). The identified proteins cover a broad range of functions such as protein degradation, protein synthesis, energy metabolism, and immune response as well as other cellular and extracellular functions. Many of the identified proteins (designated as footnote *b* in Table 1) have previously been identified in human macrophages by MALDI TOF MS (*18*−*20*), but there

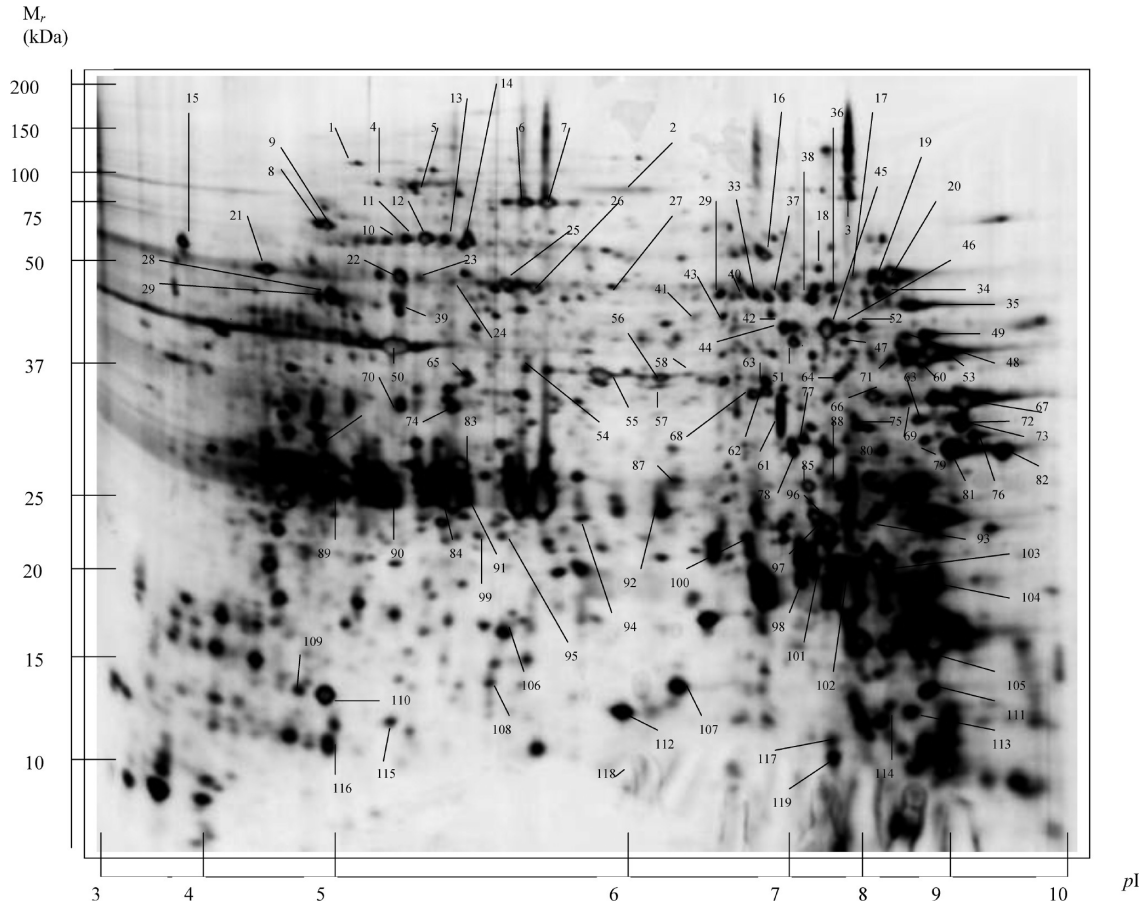

Figure 3. Representative 2-DE image of the proteome from unexposed macrophages. Proteins were separated by isoelectric focusing (3−10NL) in the first and by SDS-PAGE in the second dimension. Proteins were silver-stained, quantified, and identified by MALDI TOF MS.

are also several proteins that, to our knowledge, are identified in human macrophages for the first time.

Significant Effects of WP on the MDM Proteome. Significant effects of WP on the MDM proteome are shown in Figure 4 and listed in Table 2. Thus, 7 of the 119 identified proteins were significantly down-regulated after WP exposure, whereas 3 proteins were up-regulated. Several of the down-regulated proteins are known to be involved in energy metabolism, for example, enolase 1, ATP synthase B-chain mitochondrial precursor, acetyl-coenzyme A acyltransferase 2, and triosephosphate isomerase 1, but also proteins involved in protein degradation (26S proteasome subunit p45), protein synthesis (tryptophanyl-tRNA synthetase), and dithiol/disulfide oxidoreductase reactions (protein disulfide isomerase) were found among down-regulated proteins. By contrast, calgizzarin (marker of inflammation), galectin 3 (biomarker of fibrosis), and macrophage capping protein (macrophage function by reversible calcium-dependent blocking of actin) were found to be significantly up-regulated after WP exposure (Figure 4; Table 2).

Significant Effects of ETX on the MDM Proteome. For comparison, the effects of ETX on the MDM proteome are also shown in Figure 4 and listed in Table 2. Four proteins were significantly down-regulated after ETX exposure; two of them (Enolase 1 and 26S proteasome subunit p45) were also down-regulated after WP exposure, whereas the other two, annexin 2 (exocytosis) and fructose 1,6-bisphosphatase 1 (glycolysis), were not. Notably, the interesting two proteins, calgizzarin and galectin 3, that were found to be up-regulated after WP exposure were also up-regulated after ETX exposure (Figure 4; Table 2).

Nonsignificant Trends of ETX or WP on the MDM Proteome. Overall, proteins associated with inflammatory response were increased and proteins involved in cellular functions such as redox balance, anti-inflammatory response, and glycolysis were decreased after both exposures, but there were, in addition to the significant changes described above, also several nonsignificant changes of interest. Among others, three proteins that are known to be involved in innate immunity and activated upon bacterial challenges (*21*−*25*), cystatin B, peroxiredoxin I, and calreticulin, were found to be up-regulated in the ETX-exposed MDM cells. In contrast, after WP exposure of the MDM cells, cystatin B, peroxiredoxin I, and calreticulin were down-regulated. This finding points out that the effects on the MDM proteome after WP exposure in this study are related to factors other than ETX.

Discussion

There is no doubt that there are airborne PMs that exert deleterious effects on human cardiopulmonary health. Several previous studies have shown release of cytokines such as IL-6, IL-8, and TNF-α by both PM exposure (*13, 14*) and ETX exposure (*20*) of human macrophages. Those well-known cytokines are potent markers of increased oxidation or inflammatory response, but they are still unspecific.

Elucidating and comparing the proteomic pathways that are activated in human macrophages by exposure to PM with different characteristics such as defined size, shape, and adsorbed material, or, as in this study, one type of WP compared to ETX may contribute to the identification of more specific marker proteins or pathways. This information is crucial for the industry as well as the common population concerning future safety recommendations.

Significant Protein Alterations. Noticeable is that of the seven proteins (Figure 4; Table 2) that were significantly down-

Table 1. Proteins Identified from 2-D Gels

spot[a]	accession no. (Swiss-Prot)	protein name	function	theor M_r	theor p*I*	exptl M_r	exptl p*I*	sequence coverage (%)	peptides (no. of peaks)	MOWSE score (by MS-Fit)
1	P34932	HSP 70 protein 4, isoform A	chaperone	94.33	5.1	100	5.4	25.6	20	$4.98e^{+6}$
2	P21333	filamin 1	actin binding	88.59	5.9	94.6	5.8	29.6	16	$1.71e^{+6}$
3	Q99798	aconitase 2,[b] mitochondrial	citric acid cycle	85.57	7.6	92.8	6.8	21.2	13	$1.17e^{+6}$
4	P55072	valosin containing protein	multifunction, cell cycle, protein degradation	89.32	5.1	89.3	5.4	59.2	21	$4.00e^{+6}$
5	P19338	nucleolin	chromatin decondensation	76.34	4.6	89.1	5.5	18	15	$2.01e^{+3}$
6	P06396	gelsolin, actin depolymerizing factor	severs actin filament	80.64	5.6	80.4	5.9	34.5	23	$2.58e^{+9}$
7	P06396	gelsolin, actin depolymerizing factor	severs actin filament	80.64	5.6	80.4	6.0	29	23	$8.02e^{+5}$
8	NCBI: NP_005338	heat shock 70 kDa protein 5	chaperone	72.33	5.1	68.8	5.2	41	25	$1.78e^{+9}$
9	NCBI: NP_005338	heat shock 70 kDa protein 5	chaperone	72.33	5.1	68.8	5.2	47	29	$3.73e^{+10}$
10	Q14651	L-plastin[b]	actin bundling	70.26	5.2	64.6	5.4	43	28	$1.28e^{+13}$
11	P11142	71 kDa heat shock cognate protein,[b] HSP 70 protein 8 isoform 1	chaperone	70.90	5.4	64.6	5.4	17	11	$2.80e^{+4}$
12	P11142	71 kDa heat shock cognate protein,[b] HSP 70 protein 8 isoform 1	chaperone	70.90	5.4	64.6	5.6	53	40	$2.75e^{+16}$
13	P11142	71 kDa heat shock cognate protein,[b] HSP 70 protein 8 isoform 1	chaperone	70.90	5.4	65.6	5.6	17.2	11	$2.80e^{+4}$
14	P38646	HSP 70 kDa protein 9B precursor variant[b]	cell proliferation, aging chaperone	73.64	5.9	64.6	5.7	37.6	22	$1.46e^{+11}$
15	P27797	calreticulin[b]	calcium signaling	46.92		58.3	3.9	37	16	$7.71e^{+5}$
16	P31948	stress-induced phosphoprotein 1 (STIP1[b])	mediates chaperon association	62.64	6.4	58.3	6.9	72.9	48	$1.44e^{+12}$
17	P50995	annexin 11[b]	immune response	54.39	7.5	54.2	7.9	23	14	$2.80e^{+4}$
18	P04040	catalase	antioxidant	59.73	7.4	52.1	7.4	33	37	$6.86e^{+15}$
19	P04264	keratin 1	cytoskeletal	66.02	8.2	52.1	8.4	18	11	$2.36e^{+4}$
20	P14618	pyruvate kinase 3	glycolysis	57.98	8.4	52.1	8.5	59	30	$1.66e^{+15}$
21	P07237	protein disulfide-isomerase[b]	rearrangement of disulfide bonds inhibits NF-κB activation	57.12	4.8	50.0	4.7	52	31	$3.90e^{+11}$
22	P10809	chaperonin, heat shock protein 60 (HSP60)	protein assembly	61.06	5.7	50.0	5.4	36	19	$5.67e^{+6}$
23	P10809	chaperonin, heat shock protein 60 (HSP60)	protein assembly	61.06	5.7	50.0	5.5	47.8	22	$8.26e^{+7}$
24	P13796	L-plastin[b]	actin binding	70.29	5.3	50.0	5.6	43.7	28	$1.28e^{+13}$
25	P13796	L-plastin[b]	actin binding	70.29	5.3	50.0	5.6	38	12	$2.68e^{+5}$
26	P07237	protein disulfide-isomerase[b]	rearrangement of disulfide bonds inhibits NF-κB activation	57.12	4.8	50.0	5.7	37	23	$2.317e^{+09}$
27	P23381	tryptophanyl-tRNA synthetase (WARS)[b]	protein synthesis	48.85	6.0	48.9	5.9	71.2	6	$1.81e^{+3}$
28	P06576	ATP synthase β-chain mitochondrial precursor[b]	produces ATP from ADP	56.56	5.3	47.8	5.1	43	18	$2.32e^{+10}$
29	P06576	ATP synthase β-chain mitochondrial precursor[b]	produces ATP from ADP	56.56	5.3	47.8	5.1	34	14	$1.11e^{+8}$
30	Q8WVJ4	leukocyte-derived arginine aminopeptidase (LRAP)	proteolysis	40.06	6.7	47.8	5.9	20.6	10	$0.08e^{+3}$
31	P62068	ubiquitin specific protease 46	ubiquitin removal	42.44	6.4	46.8	5.3	8.2	6	$0.37e^{+3}$
32	P00352	aldehyde dehydrogenase 1 (ALDH1)	alcohol metabolism	54.84	6.3	46.8	6.4	41.1	21	$8.26e^{+5}$
33	P00352	aldehyde dehydrogenase 1 (ALDH1)	alcohol metabolism	54.84	6.3	46.8	6.8	29.7	15	$0.30e^{+3}$
34	P28838	leucine aminopeptidase	protein processing	56.05	7.6	46.8	7.1	88.6	68	$5.34e^{+3}$
35	P09622	dihydrolipoamide dehydrogenase	pyruvate metabolism	54.18	8.0	46.8	7.6	43.4	16	$1.50e^{+5}$
36	P00367	glutamate dehydrogenase 1 (GLUD 1)[b]	amino acid metabolism	61.34	8.1	46.8	7.7	18.8	12	$2.39e^{+3}$
37	P00390	glutathione reductase	antioxidant	51.70	7.6	46.8	8.3	30.0	15	$1.31e^{+5}$
38	P25705	ATP synthase (ATP5A1)	produces ATP from ADP	59.81	9.1	46.8	8.6	51	34	$3.33e^{+11}$
39	P19971	endothelial cell growth factor 1	cell growth	49.96	5.4	45.1	5.3	44.4	20	$5.82e^{+7}$
40	P00352	aldehyde dehydrogenase 1	alcohol metabolism	54.73	6.3	44.6	6.1	35	16	$7.43e^{+6}$
41	P02647	apolipoprotein A1[b]	cholesterol transport	30.78	5.6	44.6	6.3	45	15	$4.03e^{+5}$
42	P07339	cathepsin D[b]	lysosomal	44.55	6.1	44.5	6.2	20.6	8	$1.29e^{+3}$
43	P00352	aldehyde dehydrogenase 1	alcohol metabolism	54.73	6.3	43.5	6.6	19		
44	P06733	enolase 1 variant[b]	glycolysis, growth control, hypoxia tolerance, allergic response	47.14	7.0	43.5	7.0	43	19	$1.56e^{+14}$

Table 1. Continued

spot[a]	accession no. (Swiss-Prot)	protein name	function	theor M_r	theor p*I*	exptl M_r	exptl p*I*	sequence coverage (%)	peptides (no. of peaks)	MOWSE score (by MS-Fit)
45	P06733	enolase 1 variant[b]	glycolysis, growth control, hypoxia tolerance, allergic response	47.14	7.0	43.5	7.6	35	16	$1.16e^{+07}$
46	P06733	enolase 1 variant[b]	glycolysis, growth control, hypoxia tolerance, allergic response	47.14	7.0	43.5	7.8	17.1	7	$0.37e^{+3}$
47	P07954	fumarate hydratase	Krebs cycle	54.64	8.8	43.5	8.0	47.6	17	$1.65e^{+4}$
48	Q9NUB1	acetyl-coenzyme A acyltransferase 2	ATP synthesis	41.92	8.3	41.3	8.8	11.6	6	$0.13e^{+3}$
49	Q9NUB1	acetyl-coenzym A acyltransferase 2	ATP synthesis	41.92	8.3	41.3	9.0	42.1	17	$2.49e^{+5}$
50	P68133	cytoplasmic actin	cell motility	41.74	5.3	39.2	5.4	61	23	$1.47e^{+10}$
51	P62195	26S proteasome subunit p45	protein degradation	30.00	6.9	39.2	7.1	23	6	$0.14e^{+3}$
52	P62195	26S proteasome subunit p45	protein degradation	30.00	6.9	39.2	7.9	47.9	16	$3.83e^{+5}$
53	P00558	migration-inducing gene 10, phosphoglycerate kinase 1	glycolysis	44.62	8.3	39.2	9.0	70	31	$1.59e^{+15}$
54	P40121	macrophage capping protein[b]	macrophage functions	38.52	5.9	37.0	5.7	23.6	8	$1.20e^{+3}$
55	P40121	macrophage capping protein[b]	macrophage functions	38.52	5.9	37.0	5.9	24	10	$9.24e^{+4}$
56	P40121	macrophage capping protein[b]	macrophage functions	38.52	5.9	37.0	6.1	23.3	8	$0.74e^{+3}$
57	P40121	macrophage capping protein[b]	macrophage functions	38.52	5.9	37.0	6.1	23.3	8	$0.74e^{+3}$
58	Q00325	phosphate carrier protein (PTP)	phosphorylation	40.10	9.5	37.0	6.3	27.1	8	$2.90e^{+4}$
59	P04075	aldolase,[b] fructose 1,6-bisphosphate (ALDOA)	glycolysis	39.45	8.5	37.0	8.8	34	10	$1.19e^{+6}$
60	P04075	aldolase,[b] fructose 1,6-bisphosphate (ALDOA)	glycolysis	39.45	8.5	37.0	8.4	32	9	$4.67e^{+5}$
61	P04083	annexin 1[b]	exocytosis	38.72	6.6	36.0	6.7	55	19	$3.79e^{+6}$
62	O60218	aldo keto reductase[b]	oxidoreductase activity	36.58	6.3	36.0	6.7	54	22	$5.48e^{+8}$
63	Q9BWD1	acetyl CoA transferase 2	lipoprotein transport	41.38	6.5	36.0	6.7	35	12	$2.49e^{+5}$
64	P06733	enolase 1 variant[b]	glycolysis, growth control, hypoxia tolerance, allergic response	47.14	7.0	35.0	6.4	25	12	$1.87e^{+5}$
65	P02647	apolipoprotein A1[b]	cholesterol transport	30.79	5.6	34.3	5.4	64	18	$2.14e^{+8}$
66	P07355	annexin 2[b]	exocytosis	38.6	7.6	34.0	8.3	32.4	11	$1.03e^{+5}$
67	P04406	glyceraldehyde-3-phosphate dehydrogenase[b]	glycolysis	36.05	8.6	33.7	9.3	42.7	17	$1.98e^{+8}$
68	P09467	fructose-1,6-bisphosphatase 1	glycolysis	36.68	6.6	33.3	7.1	38	15	$3.36e^{+4}$
69	Q00526	cyclin-dependent kinase 3	cell proliferation	35.05	8.9	33.0	8.7	26.2	7	$1.82e^{+3}$
70	P07858	cathepsin B[b]	thiol protease	37.78	5.9	31.7	5.0	23	5	$0.18e^{+3}$
71	P07355	annexin 2[b]	exocytosis	38.6	7.6	31.7	8.8	48	20	$6.19e^{+10}$
72	P04406	glyceraldehyde-3-phosphate dehydrogenase	glycolysis	36.05	8.6	31.7	9.4	45	18	$3.93e^{+6}$
73	P40926	malate dehydrogenase, mitochondrial	citric acid cycle	35.50	8.9	31.7	9.4	41.4	16	$2.44e^{+4}$
74	P52907	capping protein α (CAPZA1)[b]	actin assembly, cell motility	32.92	5.4	31.3	5.5	85.7	38	$1.28e^{+7}$
75	P45880	voltage-dependent anion-selective channel protein 2	cell volume regulation, apoptosis	31.57	7.5	31.3	8.2	30	8	$6.42e^{+3}$
76	P21796	porin,[b] voltage dependent anion channel	cell volume regulation, apoptosis	30.77	8.6	29.6	9.6	28	14	$8.02e^{+5}$
77	P40925	malate dehydrogenase,[b] cytoplasmic	citric acid cycle	36.43	6.9	29.7	7.2	33	11	$2.44e^{+4}$
78	Q5T0R1	CAP,[b] adenylate cyclase-associated protein 1	formation of cAMP	28.69	7	29.3	7.2	22	7	$0.16e^{+3}$
79	O76003	thioredoxin-interacting protein	thioredoxin inhibition, redox regulation	33.62	8.8	29.0	8.8	10	4	$0.04e^{+3}$
80	P17931	galectin 3 (LGALS3)[b]	cell differentiation	26.15	8.6	28.6	8.4	25	9	$1.03e^{+3}$
81	P17931	galectin 3 (LGALS3)[b]	cell differentiation	26.15	8.6	28.6	9.4	22	6	$1.01e^{+4}$
82	P17931	galectin 3 (LGALS3[b])	cell differentiation	26.15	8.6	28.3	9.8	33	11	$3.34e^{+5}$
83	Q6PJ43	ACTG-1[b]	cell motility	29.41	5.5	27.3	5.5	32.3	8	$0.16e^{+3}$
84	Q6PJ43	ACTG-1[b]	cell motility	29.41	5.5	27.0	5.5	49	11	$0.28e^{+3}$
85	P18669	phosphoglycerate mutase[b], PGAM1	glycolysis	28.80	6.7	25.0	7.5	59	14	$4.51e^{+7}$
86	O00299	chloride intracellular channel 1[b]	chloride ion transport	26.92	5.1	25.0	5.0	34	9	$4.19e^{+3}$
87	P30040	endoplasmic reticulum protein 29[b]	protein processing	28.99	6.8	25.0	5.9	33.7	10	$4.23e^{+4}$
88	P25774	cathepsin S	elastase activity	37.50	8.6	25.0	8.0	26	8	$2.05e^{+3}$
89	Q0D2I5	Hom-Tes 103	antitumor	29.33	4.8	24.0	5.1	25.8	7	$0.18e^{+3}$
90	P02647	apolipoprotein A1[b]	cholesterol transport	30.79	5.6	24.0	5.4	45	12	$1.19e^{+6}$
91	P02647	apolipoprotein A1[b]	cholesterol transport	30.79	5.6	24.0	5.6	35	11	$1.49e^{+4}$
92	P04792	heat shock protein 27[b]	stress resistance, actin organization	22.33	7.8	24.0	5.8	39.7	8	$0.15e^{+3}$
93	P25774	cathepsin S	elastase activity	37.50	8.6	23.5	8.7	15	5	$0.24e^{+3}$
94	P62993	growth receptor bound protein	cell signaling	23.56	6.3	23.2	6.0	53.2	12	$8.69e^{+3}$
95	P02647	apolipoprotein A1,[b] isoforms CRA-a	cholesterol transport	30.79	5.6	23.0	5.7	45.7	11	$1.41e^{+5}$
96	P60174	triosephosphate isomerase 1[b]	glycolysis	26.64	6.4	23.0	7.4	71	17	$5.46e^{+7}$
97	Q9Y314	nitric oxide synthase-interacting protein	inhibitor of nitric oxide production	33.17	9.06	23	7.8	27	8	$0.20e^{+3}$
98	Q9Y314	nitric oxide synthase-interacting protein	inhibitor of nitric oxide production	33.17	9.06	21.5	7.8	22	8	$0.16e^{+3}$

Table 1. Continued

spot[a]	accession no. (Swiss-Prot)	protein name	function	theor M_r	theor p*I*	exptl M_r	exptl p*I*	sequence coverage (%)	peptides (no. of peaks)	MOWSE score (by MS-Fit)
99	P09211	glutathione *S*-transferase P[b]	glutathione conjugation	23.22	5.44	21.2	5.6	52	6	$3.19e^{+3}$
100	Q5TBC2	adaptor related protein complex 4, β 1 subunit	intracellular traffic	20.18	8.5	21.2	6.7	18.3	3	$0.02e^{+3}$
101	Q06830	peroxiredoxin 1 (PRDX 1)[b] natural killer cell enhancing factor	redox regulation	22.11	8.3	21.0	7.4	48	12	$9.30e^{+3}$
102	P04179	superoxide dismutase Mn	down-regulates oxidative stress	24.72	8.3	20.0	7.7	41.8	8	$1.68e^{+4}$
103	Q06830	peroxiredoxin 1 (PRDX 1)[b] natural killer cell enhancing factor	redox regulation	22.11	8.3	20.0	8.4	68	21	$1.57e^{+9}$
104	Q06830	peroxiredoxin 1 (PRDX 1)[b] natural killer cell enhancing factor	redox regulation	22.11	8.3	19.2	8.9	40	11	$1.10e^{+4}$
105	NCBI AAW68526	antitetanus toxoid immunoglobulin heavy chain variable region	antibody	13.58	9.3	15.4	8.4	19.7	3	$0.08e^{+3}$
106	Q13404	ubiquitin-conjugating enzyme E2 variant 1	transcriptional activation, DNA repair	11.77	5.4	15.0	5.2	45	5	0.01^{+3}
107	Q01469	fatty acid binding protein 5, epidermal (E-FABP)	lipid transport, metabolism	15.16	6.6	13.8	6.2	65	15	$1.49e^{+3}$
108	P02647	apolipoprotein AI[b]	cholesterol transport	30.79	5.6	13.4	5.7	43.8	15	$4.03e^{+5}$
109	P09382	galectin 1	cell apoptosis, differentiation	14.72	5.3	13.1	5.0	73	11	$4.05e^{+3}$
110	P20382	melanin-concentrating hormone	neurotransmitter	18.7	6.7	12.8	5.1	22	7	$0.09e^{+3}$
111	P07737	profilin 1	actin polymerization (cell motility)	15.05	8.4	12.8	8.9	75.7	12	$2.12e^{+5}$
112	P15090	fatty acid binding protein 4	lipid transport	14.72	6.6	12.5	6.0	40	4	$0.05e^{+3}$
113	P62937	cyclophilin A (peptidyl-prolyl cis-transisomerase A	protein folding	17.88	7.8	12.3	8.7	79.3	6	$5.96e^{+3}$
114	P07737	profilin 1	actin polymerization (cell motility)	15.05	8.4	12.3	8.4	72.9	12	$2.12e^{+5}$
115	P55822	SH3 domain binding glutamic acid-rich protein like (SH3BGRL)	protein−protein interaction in signal transduction	12.77	5.2	12.2	5.3	40	4	$0.06e^{+3}$
116	P45452	collagenase 3 (MMP3)	collagen degrading	13.85	5.6	11.4	5.0	39.7	7	$0.04e^{+3}$
117	P04080	cystatin B	thiol proteinase inhibitor	11.14	7.0	11.4	7.8	67	8	$6.90e^{+3}$
118	P31949	calgizzarin (S100 calcium-binding protein A11)	calcium binding	11.74	6.6	10.0	5.8	58	8	$0.37e^{+3}$
119	P62988	ubiquitin	protein degradation	8.57	6.6	8.8	7.8	72	7	1.61^{+4}

[a] Spot numbers correspond to indicated proteins in 2-D image in Figure 3. [b] Previously identified in human MDM using MALDI-TOF.

regulated by WP exposure of the MDM cells, only two (26S proteasome subunit p45 and enolase 1 involved in protein degradation and glycolysis, repectively) were also significantly down-regulated after ETX exposure. The other five proteins, involved in energy metabolism (ATP synthase B-chain mitochondrial precursor, acetyl-coenzyme A acyltransferase 2, triosephosphate isomerase 1), protein synthesis (tryptophanyl-tRNA synthetase), and dithiol/disulfide oxidoreductase reactions (protein disulfide isomerase (PDI)), did follow the same trend after ETX exposure, but not significantly. The specific importance of the down-regulation of the seven proteins is not known. However, down-regulation of proteins is most likely as important to the overall cell function as up-regulation.

In agreement with our results, PDI levels have previously been found to decrease in monocytes exposed to ETX (*20*). Interestingly, in our study, PDI was detected in two positions (Figure 3; Table 1) with the same mass but with different p*I* values (4.7 and 5.7) and WP decreased the levels for the acidic isoform, whereas ETX impaired the expression of the more basic isoform.

Galectin 3 and calgizzarin were significantly up-regulated after both WP and ETX exposure (Figure 4; Table 2). Galectin 3 is a recently developed biomarker associated with fibrosis and inflammation (*26*), and levels have been found to be increased in atherosclerotic lesions (*27*). By others, galectin 3 has also been described as a negative regulator of LPS-mediated inflammation (*28*). According to previous findings, calgizzarin (S100A11), a calcium-binding protein, is highly expressed in cancer tissues (*29*) and in cardiomyocytes during myocardial damage (*30*). Interestingly, in a recent paper, S100A11 has also been significantly up-regulated in macrophages treated with VLDL, indicating that S100A11 may be related to macrophage proliferation (*31*).

The only protein that was significantly up-regulated after WP but not ETX exposure is macrophage capping protein (MCP). MCP is a calcium-sensitive protein that has been suggested to play an important role in macrophage function and maturation by interacting with actin (*32*). Here, MCP is present as four distinct isoforms with the same molecular weight, but with different p*I* values (Figure 3; Table 1). For the isoform at p*I* 5.9, ETX has a suppressive effect, whereas WP significantly up-regulated both the p*I* 5.9 and the p*I* 6.2 isoforms. Very few studies are available concerning this protein in relation to cardiopulmonary diseases, and MCP function in relation to WP exposure needs to be further investigated to be able to draw any conclusions.

Nonsignificant Protein Alterations. Overall, among the identifications, proteins associated with inflammatory response were increased and proteins involved in cellular functions were decreased

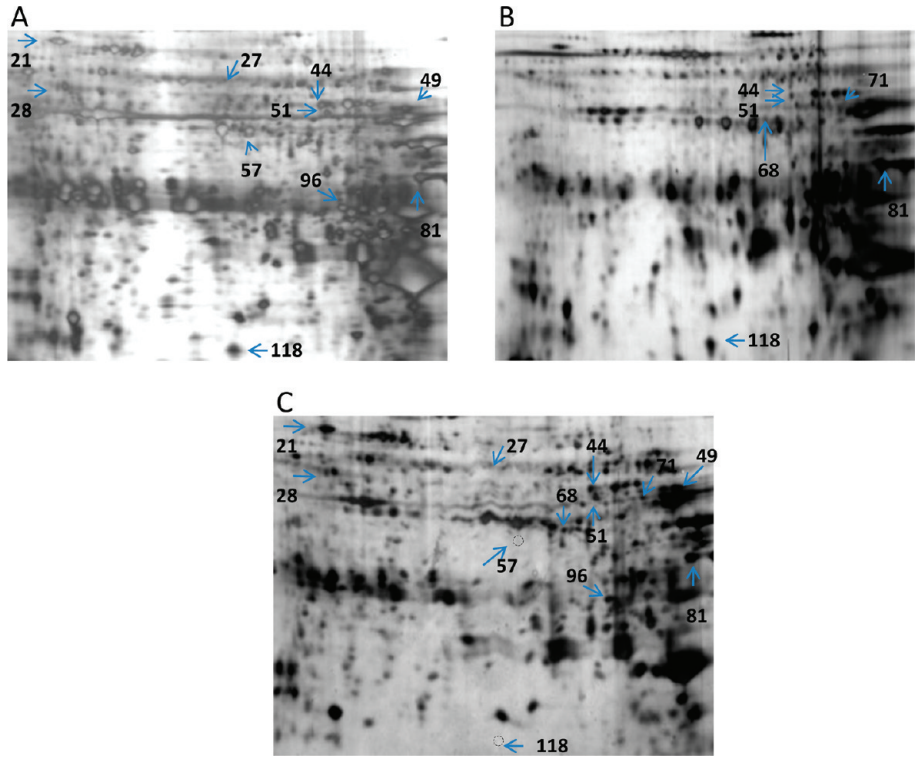

Figure 4. Protein patterns in MDM cells after exposure to WP and ETX. Marked proteins are differentially expressed in WP exposed cells (A) and/or ETX exposed cells (B) compared to controls (C), as shown in Table 2. Circles indicate the theoretical positions of very low abundant proteins in the control.

Table 2. Changes in Protein Expression after Exposure of MDM to WP or ETX, Respectively[a]

spot	protein name	control	effect by WP	*p* value	effect by ETX	*p* value
21	protein disulfide-isomerase[b]	1.54 ± 0.60	0.07 ± 0.03	↓ (0.09)	1.60 ± 0.90	
27	tryptophanyl-tRNA synthetase (WARS)[b]	0.10 ± 0.01	0.03 ± 0.02	↓ (0.03)	0.10 ± 0.03	
28	ATP synthase β-chain mitochondrial precursor[b]	0.06 ± 0.02	0.01 ± 0.01	↓ (0.09)	0.04 ± 0.02	
44	enolase 1 variant[b]	0.92 ± 0.26	0.15 ± 0.04	↓ (0.09)	0.09 ± 0.02	↓ (0.01)
49	acetyl-coenzyme A acyltransferase 2	0.88 ± 0.12	0.10 ± 0.05	↓ (0.03)	0.70 ± 0.55	
51	26S proteasome subunit p45	2.85 ± 0.62	0.83 ± 0.26	↓ (0.03)	0.52 ± 0.15	↓ (0.01)
57	macrophage capping protein[b]	0.02 ± 0.01	0.12 ± 0.05	↑ (0.06)	0.03 ± 0.01	
68	fructose-1,6-bisphosphatase 1	2.12 ± 1.16	0.12 ± 0.10		0.91 ± 0.76	↓ (0.08)
71	annexin 2[b]	0.08 ± 0.03	0.03 ± 0.03		0.01 ± 0.01	↓ (0.08)
81	galectin 3 (LGALS3)[b]	0.34 ± 0.17	2.13 ± 1.07	↑ (0.05)	2.54 ± 0.94	↑ (0.08)
96	triosephosphate isomerase 1[b]	0.09 ± 0.02	0.03 ± 0.02	↓ (0.09)	0.15 ± 0.09	
118	calgizzarin (S100 calcium-binding protein A11)	<0.01	0.03 ± 0.02	↑ (0.05)	0.33 ± 0.17	↑ (0.05)

[a] The effect of the exposure is indicated by the direction of the arrow, showing an increase or a decrease in protein expression as compared to unexposed MDM cells. Protein intensity values are mean ± SEM and expressed as percent of total protein intensity in the gel image. The significance ($p < 0.1$) is based on five different experiments. [b] Protein previously identified in macrophages.

after both WP and ETX exposure. Despite a limited number of identifications and comparisons, protein changes were found in the MDM proteome after both exposures. Because the aim was to find specific marker proteins that were differentially expressed after ETX and WP exposure and the best candidate found was MCP, also the nonsignificant protein changes are of interest.

Thus, three proteins, calreticulin, cystatin B, and peroxiredoxin I, were up-regulated after ETX but down-regulated after WP exposure compared to controls. Calreticulin is a multifunctional protein known to bind molecules of the innate immunity such as C1q. The functional implications of C1q−calreticulin interactions are still unknown. However, C1q deficiency is known to result in an increased risk for bacterial infections and autoimmune diseases; therefore, calreticulin expression may be sensitive to ETX exposure (*21, 22*). Cystatin B, a cystein proteinase inhibitor, was also differentially expressed, and our finding is thus in line with that of Lefebvre et al. (*23*), reporting gene up-regulation of cystatin B upon bacterial challenge in leech. Peroxiredoxin I has previously been suggested to stimulate the secretion of pro-inflammatory cytokines in murine macrophages (*24*), and stimulation with ETX resulted in increased expression of peroxiredoxin I mRNA in tammar leukocytes (*25*). The three described proteins may belong to pathways that do not recognize WP, or taking into account the fact that the levels are even lower in the WP-exposed MDMs compared to controls, the MDM cells may prioritize selected pathways with down-regulation of less important pathways, as a consequence.

Methodological Considerations. This study was performed using human MDM cells that in earlier investigations have been shown to resemble alveolar macrophages both morphologically and functionally in their ability to secrete pro-inflammatory cytokines (*13, 14*). Macrophages are the first inflammatory cells to encounter materials such as WP when entering the airways. Thus, understanding how these cells react is crucial to understanding the inflammatory reaction within the airways. The proteins were visualized using silver Shevchenko staining, the most sensitive method that allows identification of proteins with MALDI TOF MS. The drawback of this staining method, that saturated protein

spots are not possible to quantify, did not overcome the advantage of being able to identify also proteins of interest in low abundance. However, it is important to keep in mind that what can be visualized by staining is only a top fraction of the proteins expressed in macrophages, and it can be expected that there are still several proteins at low abundance below the detection level that have not been evaluated. Approximately the same amounts of cells were used and according to the measuring of protein concentration, the amounts of proteins (except from one WP preparation) did not differ between samples, indicating that the observed differences in protein spot intensity are related to induced variations in the protein expression.

Conclusion. Investigating the effects of characterized particles on human MDM cells in vitro, using a proteomic approach, has shown to be useful. Detailed information about protein changes that may lead to a better understanding of the underlying mechanisms in MDM cells during particle exposure has been achieved. WP and ETX exposure of the MDM cells showed similar effects but also pointed out differences in protein expression despite a limited number of observations.

Summarizing the findings allows us to suggest that galectin 3, calgizzarin, or MCP may be new possible marker proteins and the missing link between the exposures to PM, such as the WP used in this study, and cardiovascular complications.

References

(1) Sarnat, J. A., Schwartz, J., and Suh, H. H. (2001) Fine particulate air pollution and mortality in 20 U.S. cities. *N. Engl. J. Med. 344* (16), 1253–1254.

(2) Moreno, T., Querol, X., Alastuey, A., Ballester, F., and Gibbons, W. (2007) Airborn particulate matter and premature deaths in urban Europe: the new WHO guidelines and the challenge ahead as illustrated by Spain. *Eur. J. Epidemiol. 22* (1), 1–5.

(3) Oberdörster, G., Maynard, A., Donaldson, K., Castranova, V., Fitzpatrick, J., Ausman, K., Carter, J., Karn, B., Kreyling, W., Lai, D., Olin, S., Monteiro-Riviere, N., Warheit, D., and Yang, H. (2005) Principles for characterizing the potential human health effects from exposure to nanomaterials: elements of a screening strategy. *Part. Fibre Toxicol. 2*, 1–35.

(4) Wahlström, J., Olander, L., and Olofsson, U. (2010) Size, shape, and elemental composition of airborne wear particles from disc brake materials. *Tribol. Lett. 38*, 15–24.

(5) Lewtas, J. (2007) Air pollution combustion emissions: characterization of causative agents and mechanisms associated with cancer, reproductive, and cardiovascular effects. *Mutat. Res. 636* (1−3), 95–133.

(6) Masiol, M., Rampazzo, G., Ceccato, D., Squizzato, S., and Pavoni, B. (2010) Characterization of PM10 sources in a coastal area near Venice (Italy): an application of factor-cluster analysis. *Chemosphere 80* (7), 771–778.

(7) Gustafsson, M., Blomqvist, G., Gudmundsson, A., Dahl, A., Swietlicki, E., Bohgard, M., Lindbom, J., and Ljungman, A. (2008) Properties and toxicological effects of particles from the interaction between tires, road pavement and winter traction material. *Sci. Total Environ. 393* (2−3), 226–240.

(8) Benke, R. R., Hooper, D. M., Durham, J. S., Bannon, D. R., Compton, K., Necsoiu, M., and McGinnis, R. N., Jr. (2009) Measurement of airborne particle concentrations near the Sunset Crater volcano, Arizona. *Health Phys. 96* (2), 97–117.

(9) Mantecca, P., Farina, F., Moschini E., Gallinotti, D., Gualtieri, M., Rohr, A., Sancini, G., Palestini P., Camatini, M. (2010) Comparative acute lung inflammation induced by atmospheric PM and size-fractionated tire particles. *Toxicol. Lett. 198* (2), 244−254.

(10) Ohyama, M., Otake, T., Adachi, S., Kobayashi, T., and Morinaga, K. A. (2007) Comparison of the production of reactive oxygen species by suspended particulate matter and diesel exhaust particles with macrophages. *Inhal. Toxicol. 19*, 57–60.

(11) Becker, S., Soukup, J. M., Sioutas, C., and Cassee, F. R. (2003) Response of human alveolar macrophages to ultrafine, fine, and coarse urban air pollution particles. *Exp. Lung.Res. 29*, 29–44.

(12) Beck-Speier, I., Dayal, N., Karg, E., Maier, K. L., Schumann, G., Schulz, H., Semmler, M., Takenaka, S., Stettmaier, K., Bors, W., Ghio, A., Samet, J. M., and Heyder, J. (2005) Oxidative stress and lipid mediators induced in alveolar macrophages by ultrafine particles. *Free Radical Biol. Med. 38* (8), 1080–1092.

(13) Lindbom, J., Gustafsson, M., Blomqvist, G., Dahl, A., Gudmundsson, A., Swietlicki, E., and Ljungman, A. G. (2007) Wear particles generated from studded tires and pavement induces inflammatory reactions in mouse macrophage cells. *Chem. Res. Toxicol. 20* (6), 937–946.

(14) Lindbom, J., Gustafsson, M., Blomqvist, G., Dahl, A., Gudmundsson, A., Swietlicki, E., and Ljungman, A. G. (2006) Exposure to wear particles generated from studded tires and pavement induces inflammatory cytokine release from human macrophages. *Chem. Res. Toxicol. 19* (4), 521–530.

(15) Cho, D. R., Shanbhag, A. S., Hong, C.-Y., Baran, G. R., and Goldring, S. R. (2002) The role of adsorbed endotoxin in particle-induced stimulation of cytokine release. *J. Orthopaedic Res. 20*, 704–713.

(16) Lindahl, M., Svartz, J., and Tagesson, C. (1999) Demonstration of different forms of the anti-inflammatory proteins lipocortin-1 and Clara cell protein-16 in human nasal and bronchoalveolar lavage fluids. *Electrophoresis 20*, 881–890.

(17) Shevchenko, A., Wilm, M., Vorm, O., and Mann, M. (1996) Mass spectrometric sequencing of proteins silver-stained polyacrylamide gels. *Anal. Chem. 68*, 850–858.

(18) Dupont, A., Tokarski, C., Dekeyzer, O., Guihot, A. L., Amouyel, P., Rolando, C., and Pinet, F. (2004) Two-dimensional maps and databases of the human macrophage proteome and secretome. *Proteomics 4*, 1761–1778.

(19) Slomianny, M. C., Dupont, A., Bouanou, F., Beseme, O., Guihot, A. L., Amouyel, P., Michalski, J. C., and Pinet, F. (2006) Profiling of membrane proteins from human macrophages: comparison of two approaches. *Proteomics 6*, 2365–2375.

(20) Gadgil, H. S., Pabst, K. M., Giorgianni, F., Umstot, E. S., Desiderio, D. M., Beranova-Giorgianni, S., Gerling, I. C., and Pabst, M. J. (2003) Proteome of monocytes primed with lipopolysaccharide: analysis of the abundant proteins. *Proteomics 3* (9), 1767–1780.

(21) Kishore, U., Sontheimer, R. D., Sastry, K. N., Zaner, K. S., Zappi, E. G., Hughes, G. R., Khamashta, M. A., Strong, P., Reid, K. B., and Eggleton, P. (1997) Release of calreticulin from neutrophils may alter C1q-mediated immune functions. *Biochem. J. 322*, 543–550.

(22) Yamada, M., Oritani, K., Kaisho, T., Ishikawa, J., Yoshida, H., Takahash, I., Kawamoto, S., Ishida, N., Ujiie, H., Masaie, H., Botto, M., Tomiyama, Y., and Matsuzawa, Y. (2004) Complement C1q regulates LPS-induced cytokine production in bone marrow-derived dendritic cells. *Eur. J. Immunol. 34*, 221–230.

(23) Lefebvre, C., Cocquerelle, C., Vandenbulcke, F., Hot, D., Huot, L., Lemoine, Y., and Salzet, M. (2004) Transcriptomic analysis in the leech Theromyzon tessulatum: involvement of cystatin B in innate immunity. *Biochem. J. 380*, 617–625.

(24) Riddell, J. R., Wang, X. Y., Minderman, H., and Gollnick, S. O. (2010) Peroxiredoxin 1 stimulates secretion of proinflammatory cytokines by binding to *TLR4*. *J. Immunol. 184*, 1022–1030.

(25) Daly, K. A., Lefévre, C., Nicholas, K., Deane, E., and Williamson, P. (2008) Characterization and expression of peroxiredoxin 1 in the neonatal tammar wallaby (*Macropus eugenii*). *Comp. Biochem. Physiol., Part B 149*, 108–119.

(26) Lok, D. J. A., Van Der Meer, P., Bruggink-André de la Porte, P. W., Lipsic, E., Van Wijngaarden, J., Hillege, H. L., and Van Veldhuisen, D. J. (2010) Prognostic value of galectin-3, a novel marker of fibrosis, in patients with chronic heart failure: data from the DEAL-HF study. *Clin. Res. Cardiol. 99* (5), 323–328.

(27) Nachtigal, M., Al-Assaad, Z., Mayer, E. P., Kim, K., and Monsigny, M. (1998) Galectin 3 expression in human atherosclerotic lesions. *Am. J. Pathol. 152*, 1199–1208.

(28) Lui, Y., Komai-Koma, M., Gilchrist, D. S., Hsu, D. K., Liu, F.-T., Springall, T., and Xu, D. (2008) Galectin 3 is a negative regulator of lipopolysaccharide mediated inflammation. *J. Immunol. 181*, 2781–2789.

(29) Ohuchida, K., Mizumoto, K., Ohhashi, S., Yamaguchi, H., Konomi, H., Nagai, E., Yamaguchi, K., Tsuneyoshi, M., and Tanaka, M. (2006) S100A11, a putative tumor suppressor gene, is over-expressed in pancreatic carcinogenesis. *Clin. Cancer Res. 15*, 5417–5422.

(30) Inamoto, S., Murao, S., Yokoyama, M., Kitazawa, S., and Maeda, S. (2000) Isoproterenol-induced myocardial injury resulting in altered S100A4 and S100A11 protein expression in the rat. *Pathol. Int. 50*, 480–485.

(31) Lu, Y., Guo, J., Di, Y., Zong, Y., Qu, S., and Tian, J. (2009) Proteomic analysis of the triglyceride rich lipoprotein-laden foam cells. *Mol. Cells 28*, 75–181.

(32) Dabiri, G. A., Young, C. L., Rosenbloom, J., and Southwick, F. S. (1992) Molecular cloning of human macrophage capping protein cDNA. A unique member of the gelsolin/villin family expressed primarily in macrophages. *J. Biol. Chem. 267* (23), 16545–16552.

TX100281F